Using active gain to maximize light absorption

Jie Wang,[1] Dezhuan Han,[2] Ang Chen,[1] Yunyun Dai,[1] Ming Zhou,[3] Xinhua Hu,[4] Zongfu Yu,[3] Xiaohan Liu,[1,5,*] Lei Shi,[1,5,†] and Jian Zi[1,5,‡]

[1]*Department of Physics, Key Laboratory of Micro- and Nano-Photonic Structures (MOE), and State Key Laboratory of Surface Physics, Fudan University, Shanghai 200433, China*

[2]*Department of Applied Physics, Chongqing University, Chongqing 400044, China*

[3]*Department of Electrical and Computer Engineering, University of Wisconsin, Madison, Wisconsin 53705, USA*

[4]*Department of Materials Science, Fudan University, Shanghai 200433, China*

[5]*Collaborative Innovation Center of Advanced Microstructures, Nanjing 210093, China*

(Received 21 August 2017; revised manuscript received 27 October 2017; published 13 November 2017)

Using an optical nanoresonator, such as a nanoparticle, to concentrate and absorb light at deep subwavelength scale is of both fundamental and technological significance. To quantify absorption, one typically introduces the absorption cross section and the absorption efficiency, i.e., the ratio of the absorption cross section of a local resonator to its geometric cross section. Exploring a general way to enlarge the absorption cross section of a deep subwavelength nanoparticle and increase the absorption efficiency certainly is important and highly desired. In this work, we show that by introducing a gain medium in the structure, the absorption cross section of any deep subwavelength particle could be boosted and even approach a universal maximum value, of the order λ^2. Our approach for controlling the absorption using gain is general and may be useful both for the design of light harvesting materials and high-speed active nano-optics devices.

DOI: 10.1103/PhysRevB.96.195419

I. INTRODUCTION

Light absorption by deep subwavelength metallic particles, due to localized plasmon resonances [1], is of great importance to many applications such as photothermal material [2–4] and plasmon-induced photovoltaic device [5,6]. To further improve the absorption performance, it is important to increase the ratio of the absorption cross section of the particle to its geometric cross section. The larger the ratio is, the higher the efficiency of light absorption could be and the less materials would be consumed as well. Typically, for a deep subwavelength gold spherical nanoparticle whose diameter is 40 nm, the absorption efficiency [7] around the plasmon resonance in visible range is about 4. For graphene nanodisk [8], whose plasmon resonance frequency falls in the midinfrared region, the efficiency is about 5. Larger absorption cross sections in metallic nanorods [9] and composite core-shell particles [10,11] are also reported. While, in the face of numerous reported absorption values of plasmonic materials with different geometries, it is important to find out a physical picture behind those detailed geometric parameters, as well as a general way to *in situ* control and enhance the absorption performance of any deep subwavelength resonator without changing their shapes. Interestingly, recalling the field of atomic physics [12], it is well known that an atom, no matter which element is, has a well-defined maximum resonant light absorption cross section, about $\lambda_0^2/4\pi$. This certainly implies that, for any deep subwavelength plasmonic particle, an optimized, even universal, absorption cross section with higher absorption efficiency similar to the value of an atom could be approached [13].

Gain, which is intuitively opposite to the absorption, has been widely applied to realize lossless plasmonic or metamaterials [14] and even plasmonic laser [15]. In those fields, people are always interested in the case that gain fully compensates the loss due to intrinsic absorption. In the present work, the effect of the gain on the absorption properties of various deep subwavelength plasmonic materials, including metallic nanoparticle and graphene nanoribbon, is reinvestigated both theoretically and numerically in detail. Surprisingly, it is found that gain can be actually used to boost the absorption performance and even approach a universal maximum absorption cross section. And importantly, the gain coefficient required to maximize absorption is less than the threshold of plasmon amplification and plasmon lasing. In principle, this work suggests a general method to realize maximum absorption cross section of any deep subwavelength absorbing particles combined with active gain medium.

II. PHYSICAL PICTURE OF MAXIMUM ABSORPTION CROSS SECTION

To understand the physical mechanism of using gain to maximize the absorption cross section, we first briefly discuss the key factors in absorption performance of plasmonic materials. Because here we focus on the deep subwavelength case, only electric dipole resonance mode excitation is taken into account. For a plane electromagnetic wave incident on a particle, part of the incident light couples to a certain resonance mode and is trapped inside the particle for a certain time. Such trapped light would have two decay channels. One is absorption by the particle, namely absorption part, and the other is reradiation to the free space, namely scattering part. Both absorption and scattering parts have their own decay rate, represented as γ_a and γ_s, respectively. A low γ_s means weak coupling between particle resonance mode and free space light mode. This weak coupling also corresponds to

*Corresponding author: liuxh@fudan.edu.cn
†Corresponding author: lshi@fudan.edu.cn
‡Corresponding author: jzi@fudan.edu.cn

less light trapped inside the particle, because the incident light mode would also couple the particle resonance mode weakly. It certainly depresses the absorption performance. On the other hand, if γ_s is high, even though the coupling is strong, the trapping time of the incident light would be too short to be absorbed by the particle, which also results in a poor absorption. Intuitionally thinking, there might be a critical relationship between γ_a and γ_s to maximize the absorption performance. Actually, based on the coupled-mode theory (CMT), this critical condition can be easily derived [16–19]. Here, we only go through the main results and leave the details of CMT to the Supplemental Material [20]. Consider a nanoresonator in the continuous medium with a refractive index n; the dynamic equations for amplitude a of resonance can be written in the following form:

$$\frac{da}{dt} = -i\omega_0 a - \gamma_a a - \gamma_s a + \boldsymbol{D}^T \mathbf{S}_{\text{in}}, \tag{1}$$

$$\mathbf{S}_{\text{out}} = \boldsymbol{C}\mathbf{S}_{\text{in}} + a\boldsymbol{D}. \tag{2}$$

The vectors $\mathbf{S}_{\text{in}}$, $\mathbf{S}_{\text{out}}$, and $\boldsymbol{D}$, whose dimension N is corresponding to the total number of channels in the free space, are the amplitude of the flux of incoming and outgoing plane waves through each channel as well as the coupling rate to each channel, respectively. The scattering matrix $\boldsymbol{C}$ describes the direct transmission between the incoming and outgoing waves. Due to the constraints of energy conservation and reciprocal theorem [21], $\boldsymbol{D}^+\boldsymbol{D} = 2\gamma_s$ and $\boldsymbol{C}\boldsymbol{D}^* = -\boldsymbol{D}$. For a dipolar resonator, the element of $\boldsymbol{D}$ is given by $\gamma_j^{\text{d}} = \sqrt{\frac{3\gamma_s}{2N_{3\text{D}}\cos\theta_j}(1-\sin^2\theta_j\cos^2\phi_j)}$, where θ_j is the polar angle and ϕ_j is the azimuth angle with respect to the channel $j(j = 1,2,\ldots,N_{3D})$. For a nanoresonator, the absorption and scattering cross sections can be derived as (see Supplemental Material [20])

$$\sigma_a = \frac{3\lambda_0^2}{2\pi n^2}\frac{\gamma_a\gamma_s}{(\omega-\omega_0)^2+(\gamma_a+\gamma_s)^2}, \tag{3}$$

$$\sigma_s = \frac{3\lambda_0^2}{2\pi n^2}\frac{\gamma_s^2}{(\omega-\omega_0)^2+(\gamma_a+\gamma_s)^2}. \tag{4}$$

It is clear that, when $\gamma_a = \gamma_s$, a critical condition is satisfied. The σ_a, at the resonant frequency ω_0, goes to its maximum

$$\sigma_a^{\max} = \frac{3\lambda_0^2}{8\pi n^2}. \tag{5}$$

As long as $\gamma_a \neq \gamma_s$, the absorption cross section must be smaller than its maximum value. If $\gamma_a < \gamma_s$, the scattering process is dominant ($\sigma_a < \sigma_s$), while if $\gamma_a > \gamma_s$, the absorption process is dominant ($\sigma_a > \sigma_s$). Note that both two cases do not reach the maximum absorption because of the mismatch between these two rates. At the last of this part, it is worth mentioning that, via Mie theory, the same maximum value can be also obtained (the details shown in the Supplemental Material [20]).

III. USING GAIN TO INCREASE ABSORPTION OF A SINGLE GOLD NANOPARTICLE

Figure 1(a) shows the γ_a and the γ_s of several gold nanospheres with different diameters from 10 nm to 80 nm

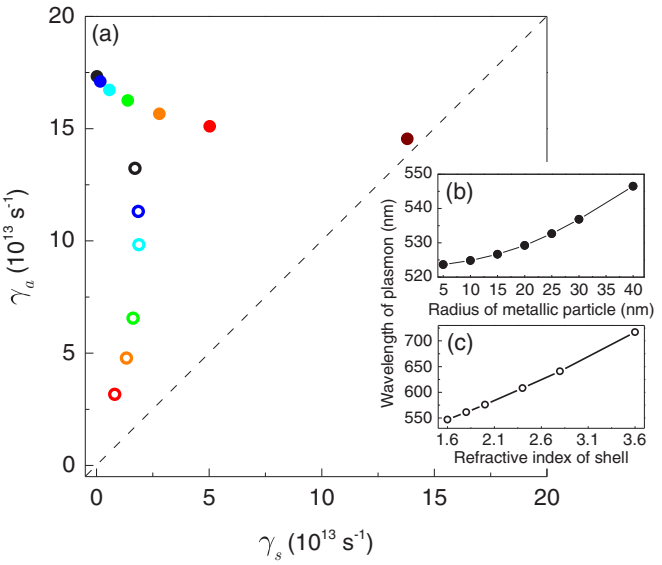

FIG. 1. (a) Solid black, blue, light blue, green, orange, red, and dark red dots represent a single gold sphere with diameter 10 nm, 20 nm, 30 nm, 40 nm, 50 nm, 60 nm, and 80 nm, respectively. Hollow black, blue, light blue, green, orange, and red dots represent a core-shell gold particle with the shell refractive index of 1.6, 1.8, 2.0, 2.4, 2.8, and 3.6, respectively; the core diameter and the shell thickness of all core-shell particles are 40 nm and 10 nm. (b) Wavelength of plasmon resonance versus radius of a metallic particle. (c) Wavelength of plasmon resonance versus refractive index of the shell of a core-shell gold particle. The diameter of the gold core and the thickness of the shell are the same as (a).

(solid dots) immersed in water, and Fig. 1(b) shows the corresponding resonant wavelength of those nanogold spheres as a function of the sphere radius. Here, γ_a and γ_s are calculated by Mie and CMT (details shown in the Supplemental Material [20]). Obviously, when the particle diameter is much smaller than the resonant wavelength (e.g., $d < \lambda/10$), $\gamma_a > \gamma_s$. For instance, in the case of 40 nm gold sphere immersed in water, whose resonant wavelength is about 530 nm, its γ_a is 10 times higher than its γ_s. The results of metallic core with dielectric shell nanosphere are also shown in Fig. 1(a) (decay rates shown as hollow dots) and Fig. 1(c) (resonant wavelength as a function of refractive index of the dielectric shell). They are similar to the pure metal particles. From the above analysis, this inequality of γ_a and γ_s results in the absorption cross section of a deep subwavelength metallic plasmonic structure far away from its maximum value. To realize $\gamma_a = \gamma_s$ [dashed line shown in Fig. 1(a)] and approach the maximum value of absorption cross section, two potential methods could be addressed. One is to increase γ_s by adjusting the particle size and geometry. Unluckily, because of the deep subwavelength nature, it is difficult to control γ_s for those tiny plasmonic structures. The other one is to decrease γ_a. As γ_a is directly related to the intrinsic material properties, it seems that it is also difficult to change. Nevertheless, it can be shown below that with a thin layer of active gain medium, γ_a of a deep subwavelength plasmonic structure can be easily adjusted to satisfy the condition ($\gamma_a = \gamma_s$) and to optimize the absorption performance. Figure 2 shows the absorption

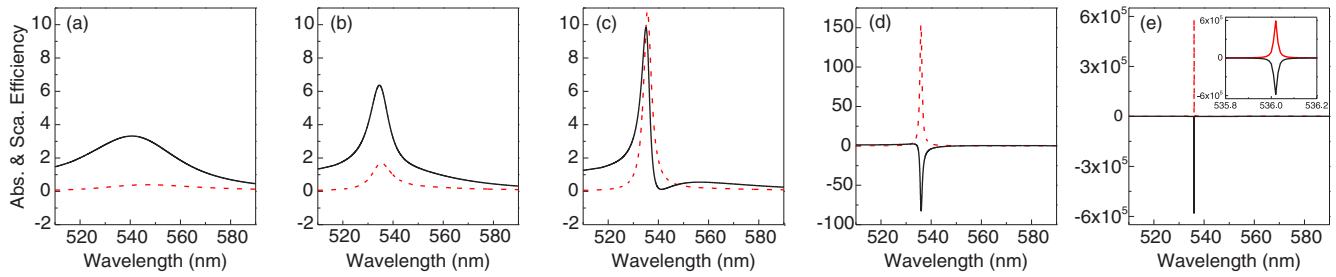

FIG. 2. (a)–(e) Black curves correspond to the absorption and red dash curves correspond to the scattering. From (a) to (e), the gain coefficients are 0 cm^{-1}, 8.24×10^4 cm^{-1}, 11.75×10^4 cm^{-1}, 13.64×10^4 cm^{-1}, and 14.36×10^4 cm^{-1}, respectively. The diameter of all gold cores is 40 nm. The shell thickness is 5 nm. Inset in (e): detailed spectra of (e) around resonant peak.

efficiency $[\sigma_a/(\pi r^2)]$ and the scattering efficiency $[\sigma_s/(\pi r^2)]$ of a gold core coated with a layer dielectric shell with gain medium for different gain coefficients. Here, the radius r of the whole particle is 25 nm and the shell thickness is 5 nm. The refractive index of the gold is adopted from the reported experimental data. The environmental medium is assumed as water with refractive index of 1.33. It is supposed that there is gain medium inside the dielectric shell. The frequency dependent dielectric constant ε of the shell material with gain is described by the Lorentz model (details shown in the Supplemental Material [20]). To show the feasibility of the gain level, the gain coefficient, $g = (4\pi/\lambda)\mathrm{Im}(\sqrt{\varepsilon})$, is shown below. For $g = 0$ cm^{-1} [Fig. 2(a)], the result is trivial. The absorption cross section (black solid line) around the resonance peak is less than the value of maximum absorption cross section and only three times larger than the value of the geometric cross section of the core-shell sphere. Also, due to its deep subwavelength size, the scattering cross section (red dashed line) is even negligible. These observations are consistent to the traditional knowledge about the optical properties of tiny plasmonic particles, specifically $\sigma_a \gg \sigma_s$. With the gain coefficient increased to 8.24×10^4 cm^{-1} [Fig. 2(b)], both absorption cross section and scattering cross section are evidently increased. As $g = 11.75 \times 10^4$ cm^{-1}, absorption cross section reaches its maximum value, as large as 10 times of its geometric cross section of the core-shell sphere [Fig. 2(c)]. Further increasing the gain coefficient, the scattering cross section increases continuously, but the absorption cross section decreases to negative value [Fig. 2(d)]. It is understandable that after certain gain level, the absorption is fully compensated by the gain, meaning amplification [Fig. 2(e)]. Finally, around $g = 14.36 \times 10^4$ cm^{-1}, the absolute value of the negative absorption cross section (or the amplification cross section) is the same as the huge scattering cross section, and the linewidth of the curves drastically drops to about 0.02 nm. These features indicate the initiation of lasing [22,23]. Figure 3(a) summarizes the results shown in Fig. 2 and shows the peak value of absorption (black) and scattering (red) efficiency at resonant wavelength as a function of gain coefficient. A maximum absorption cross section about 10 times that of the geometric section appears. And this maximum value agrees quite well with the maximum absorption cross section predicted theoretically by $\sigma_a^{\max} = (3\lambda_0^2)/(8\pi n^2)$. The absorption rate and the scattering rate of the core-shell spheres for different gain coefficients calculated based on the results shown in Fig. 2 are shown in Fig. 3(b). Before gain happened, the scattering rate γ_s is low, while γ_a is high. After introducing gain to the system, the photons coupled to the resonant mode of the particle would make more photons generated, resulting in effectively slowing down the absorption. Truly, with gain, the obtained γ_a decreases, yet the γ_s nearly stays unchanged [shown in Fig. 3(b)]. At a certain point, the absorption rate γ_a, only about 5% of the absorption decay rate without gain, reaches the value of the scattering rate γ_s. Therefore, the absorption cross section has been maximized. Continuously increasing the gain coefficient, the absorption rate further decreases and becomes less than the scattering rate. Thus again the absorption cross section is less than its maximum value. Passing through the point where $\gamma_a \sim 0$, the absorption rate goes to negative, corresponding to the negative absorption cross section $\gamma_a < 0$. It is just the amplification. Finally, the absolute value of the negative absorption rate, i.e., the amplification rate, approaches the scattering rate. It directly meets the condition of the initiation of lasing, which is the total decay rate $\gamma = \gamma_a + \gamma_s$ of the system nearly zero, namely lossless [22,23]. By Figs. 2 and 3, the effects of the gain on absorption and scattering of a deep subwavelength particle are fully expressed. Interestingly, it is worth mentioning that the critical point for maximizing the absorption cross section, $\gamma_a = \gamma_s$, is just the mirror image of the lasing point, $-\gamma_a = \gamma_s$. In other words, the present method to realize maximum absorption cross section could

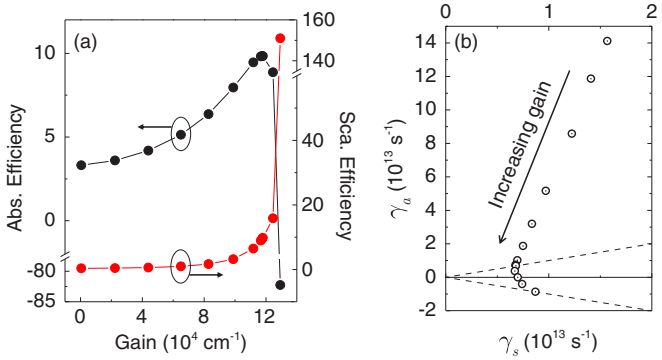

FIG. 3. (a) Peak value of absorption (black) and scattering (red) efficiency at resonant wavelength versus gain coefficient of shell material. (b) Absorption rate γ_a and scattering rate γ_s of a core-shell sphere for different gain coefficients. The arrow direction shows the trend of gain increasing. Parameters of the core-shell gold particle are the same as Fig. 2.

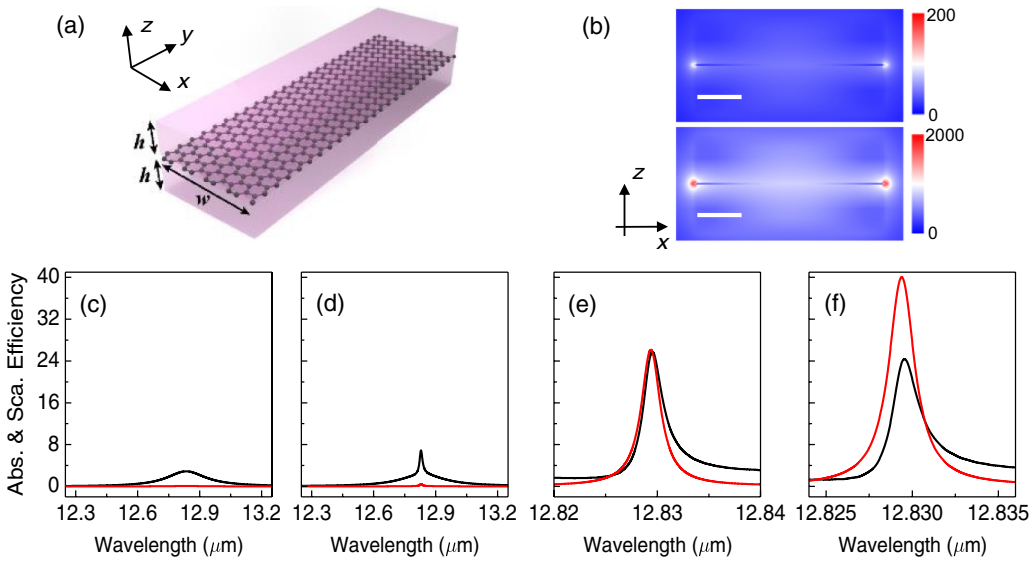

FIG. 4. (a) Schematic view of a graphene nanoribbon coated with gain dielectric layers. (b) The amplitude of electric-field distributions of the graphene nanoribbon without gain (upper) and with gain coefficient of 1.98×10^4 cm^{-1} (lower) at resonance wavelength. The scale bar is 40 nm. (c)–(f) Absorption (black) and scattering (red) efficiency (σ/w) versus wavelength for different gain coefficients 0 cm^{-1}, 1.25×10^2 cm^{-1}, 1.98×10^2 cm^{-1}, and 2.0×10^2 cm^{-1}, respectively.

also be used to realize plasmonic coherent perfect absorber or the so-called time-reversed lasing, i.e., gain would be inversed to absorption [24], $\varepsilon(r) \rightarrow \varepsilon^*(r)$.

IV. USING GAIN TO INCREASE ABSORPTION OF A GRAPHENE NANORIBBON

After the case of deep-subwavelength metallic plasmonic materials, using gain medium to boost the absorption of graphene plasmon materials is discussed. One main feature of the graphene plasmonic materials [25] is that its plasmon frequency can expand down to the midinfrared region. A graphene disk with only tens of nanometer diameter under mild doping level can support well-defined plasmon resonance around the wavelength of tens of micrometer [26–28]. According to the above discussions, it can be concluded that compared with its geometrical dimension, the maximum absorption cross section of a single graphene nanostructure should be extremely huge, because the maximum absorption cross section is proportional to λ_0^2. And the corresponding absorption efficiency, more or less in the order of $\lambda_0^2/r^2 \sim 10^4$, is even higher than that of nearly all metallic plasmonic materials. However, up to now, the reported value of the absorption cross section of a single graphene plasmonic material in normal dielectric medium is only 5, several orders less than the maximum value [8].

Figure 4(a) shows a schematic view of the investigated graphene nanoribbon with infinite length in vacuum. The width (w) of the ribbon is 160 nm. Both the upper and lower surfaces of graphene are coated with a thin dielectric layer with gain. The thickness of the gain layer is 30 nm. The frequency dependent dielectric constant of the gain layer is assumed as the same Lorentz type as mentioned above (details shown in the Supplemental Material [20]). The graphene thickness and its optical conductivity are set the same as Ref. [29]. The Fermi level of the graphene is 0.4 eV and the relaxation time is 0.4 ps. The absorption cross section and scattering cross section are calculated by a finite-difference time-domain method (FDTD). The two-dimensional FDTD simulation region is 100 μm $\times$ 100 μm. Within the area of the graphene ribbon, the smallest mesh is 0.2 nm. The simulation time is 2×10^5 fs. The plane wave source was set to have propagation direction along with the z axis and its linear electric polarization parallel to the x direction.

Figures 4(c)-4(f) show the obtained absorption (black) and the scattering (red) efficiency (σ/w) as a function of wavelength for different gain coefficients. Without gain, the absorption efficiency is only about 3. The huge difference between the absorption and scattering efficiency, indicating the large mismatch of absorption and scattering rates $\gamma_a \gg \gamma_s$, well explains the reason for the small absorption cross section compared to its theoretical maximum value. However, with gain, the absorption cross section increases rapidly as expected. Even the gain coefficient is only about 1.98×10^2 cm^{-1}; the absorption cross section, around 4 μm, approaches the maximum value of the two-dimensional dipole case, $\lambda_0/\pi \approx 12.83/3.14$ μm ≈ 4.1 μm, and the absorption efficiency is about 25. Interestingly, for the same gain coefficient, the scattering efficiency is about 100 times larger than that without gain, which is important for the coupling between different graphene nanostructures. Moreover, with gain, the local field enhancement significantly increases by one order of amplitude [see Fig. 4(b)]. These results would have great potential applications in surface enhanced infrared absorption.

V. CONCLUSION

In conclusion, a general method to control and maximize the absorption cross section of a deep subwavelength plasmonic material using a gain material is proposed and verified theoretically. The maximum absorption cross

section [$\sigma_a^{\max} = (3\lambda_0^2)/(8\pi n^2)$] is demonstrated in the visible frequency region with a modest gain coefficient of the order of 10^4. The related physical mechanism of adjusting absorption and scattering decay rate by gain is also analyzed in detail. Moreover, the method has been further applied to boost the absorption and the local field enhancement of a single graphene nanoribbon in the midinfrared region. This work shows that the absorption cross section of a nano-two-dimensional system such as free-standing graphene nanoplasmonic structure can be as high as the order of resonance wavelength. Finally, it would be emphasized that here the required gain coefficient is much less than that for amplification and lasing. Therefore, mild light could even be used to control light in nanoscale or realize a high speed nanoscale electro-optic modulator. Furthermore, thermal light radiation is proportional to the absorption and the nanoscale heat transfer can even be controlled actively.

ACKNOWLEDGMENTS

The work was supported by 973 and China National Key Basic Research Program (Grants No. 2015CB659400, No. 2016YFA0301100, and No. 2016YFA0302000), NSFC (Grants No. 11404064, No. 11774063, and No. 11727811), and the Fundamental Research Funds for the Central Universities (Grant No. CQDXWL-2014-Z005). The research of L.S. was further supported by Science and Technology Commission of Shanghai Municipality (Grant No. 17ZR1442300), state key laboratory of surface physics (Grants No. ZA2014-01 and No. KF2015-04), Professor of Special Appointment (Eastern Scholar) at Shanghai Institutions of Higher Learning, and the Recruitment Program of Global Youth Experts (1000 plans).

J.W. and D.H. contributed equally to this work.

[1] W. A. Murray and W. L. Barnes, Adv. Mater. **19**, 3771 (2007).
[2] O. Neumann, C. Feronti, A. D. Neumann, A. J. Dong, K. Schell, B. Lu, E. Kim, M. Quinn, S. Thompson, N. Grady, P. Norderlander, M. Oden, and N. J. Halas, Proc. Natl. Acad. Sci. USA **110**, 11677 (2013).
[3] Z. Y. Fang, Y. R. Zhen, O. Neumann, A. Polman, F. J. G. de Abajo, P. Nordlander, and N. J. Halas, Nano Lett. **13**, 1736 (2013).
[4] X. Zhu, C. Vannahme, E. Højlund-Nielsen, N. A. Mortensen, and A. Kristensen, Nat. Nanotechnol. **11**, 325 (2016).
[5] M. W. Knight, H. Sobhani, P. Nordlander, and N. J. Halas, Science **332**, 702 (2011).
[6] M. L. Brongersma, P. Nordlander, and N. J. Halas, Nat. Nanotechnol. **10**, 25 (2015).
[7] D. D. Evanoff, Jr. and G. Chumanov, J. Phys. Chem. B **108**, 13957 (2004).
[8] S. Thongrattanasiri, F. H. L. Koppens, and F. J. G. de Abajo, Phys. Rev. Lett. **108**, 047401 (2012).
[9] G. S. He, J. Zhu, K. Yong, A. Baev, H. Cai, R. Hu, Y. Cui, X. Zhang, and P. N. Prasad, J. Phys. Chem. C **114**, 2853 (2010).
[10] V. Grigoriev, N. Bonod, J. Wenger, and B. Stout, ACS Photon. **2**, 263 (2015).
[11] C. Tserkezis, N. Stefanou, M. Wubs, and N. A. Mortensen, Nanoscale **8**, 17532 (2016).
[12] C. J. Foot, *Atomic Physics* (Oxford University Press, Oxford, 2004).
[13] R. Fleury, J. Soric, and A. Alù, Phys. Rev. B **89**, 045122 (2014).
[14] O. Hess, J. B. Pendry, S. A. Maier, R. F. Oulton, J. M. Hamm, and K. L. Tsakmakidis, Nat. Mater. **11**, 573 (2012).
[15] M. A. Noginov, G. Zhu, A. M. Belgrave, R. Bakker, V. M. Shalaev, E. E. Narimanov, S. Stout, E. Herz, T. Suteewong, and U. Wiesner, Nature (London) **460**, 1110 (2009).
[16] Z. C. Ruan and S. H. Fan, Phys. Rev. Lett. **105**, 013901 (2010).
[17] Z. C. Ruan and S. H. Fan, Appl. Phys. Lett. **98**, 043101 (2011).
[18] R. E. Hamam, A. Karalis, J. D. Joannopoulos, and M. Soljačić, Phys. Rev. A **75**, 053801 (2007).
[19] M. Zhou, L. Shi, J. Zi, and Z. F. Yu, Phys. Rev. Lett. **115**, 023903 (2015).
[20] See Supplemental Material at http://link.aps.org/supplemental/10.1103/PhysRevB.96.195419 for detailed theoretical derivation and simulation method.
[21] S. H. Fan, W. Suh, and J. D. Joannopoulos, J. Opt. Soc. Am. A **20**, 569 (2003).
[22] Z. Y. Li and Y. N. Xia, Nano Lett. **10**, 243 (2010).
[23] S. Y. Lin, J. F. Li, F. Zhou, L. Gan, and Z. Y. Li, Opt. Lett. **36**, 1296 (2011).
[24] H. Noh, Y. D. Chong, A. D. Stone, and H. Cao, Phys. Rev. Lett. **108**, 186805 (2012).
[25] F. J. G. de Abajo, ACS Photon. **1**, 135 (2014).
[26] H. G. Yan, T. Low, W. J. Zhu, Y. Q. Wu, M. Freitag, X. S. Li, F. Guinea, P. Avouris, and F. N. Xia, Nat. Photon. **7**, 394 (2013).
[27] Z. Y. Fang, Y. M. Wang, A. E. Schlather, Z. Liu, P. M. Ajayan, F. J. G. de Abajo, P. Norderlander, X. Zhu, and N. J. Halas, Nano Lett. **14**, 299 (2014).
[28] M. S. Jang, V. W. Brar, M. C. Sherrott, J. J. Lopez, L. Kim, S. Kim, M. Choi, and H. A. Atwater, Phys. Rev. B **90**, 165409 (2014).
[29] Y. Y. Dai, A. Chen, Y. Y. Xia, D. Z. Han, X. H. Liu, L. Shi, and J. Zi, Opt. Express **24**, 20021 (2016).

Supplemental Material

I. Derivation of σ_a in 3-dimensional space with coupled-mode theory (CMT)

Consider a deep subwavelength nanoresonator in the free space with index n. Without loss of generality, we assume the incident wave propagates along z-axis and the electric field polarizes along x-axis, as shown in Fig. S1(a). With periodicity of L in the x- and y-directions, the finite number of channels in k-space is shown in Fig. S1(b). Thus, a set of coupled-mode equations can be given by[1]

$$\frac{\mathrm{d}a}{\mathrm{d}t} = -i\omega_0 a - \gamma_a a - \gamma_s a + \boldsymbol{D}^T \mathbf{S}_{\mathrm{in}}, \tag{S.1}$$

$$\mathbf{S}_{\mathrm{out}} = \boldsymbol{C}\mathbf{S}_{\mathrm{in}} + a\boldsymbol{D}, \tag{S.2}$$

with $\boldsymbol{D}$, $\mathbf{S}_{\mathrm{in}}$ and $\mathbf{S}_{\mathrm{out}}$ three $N_{3\mathrm{D}}$-dimensional vectors, where $N_{3\mathrm{D}} = 2\pi\lfloor nL/\lambda_0 \rfloor^2$ is the total number of channels and $\lfloor ... \rfloor$ is the floor operator that gives the largest integer. Moreover, the wave-vector $\mathbf{k}_\parallel$ in xy-plane is decided by $k_\parallel^2 = k^2 \sin^2\theta_j = (\frac{2\pi}{L})^2(p^2+q^2)$, where θ_j is the polar angle with respect to the channel j ($j = 1, 2, \cdots, N_{3D}$).

Suppose the mode, $a = a_0 e^{-i\omega t}$, and the amplitude a is obtained by

$$a = \frac{\boldsymbol{D}^T \mathbf{S}_{\mathrm{in}}}{-i(\omega - \omega_0) + \gamma_a + \gamma_s}. \tag{S.3}$$

The power[2] of the incidence light is $I_0 L^2 \cos 0$, while that of the jth channel is $I_j L^2 \cos\theta_j$, where the radiation I_j for the jth channel is proportional to radiative rate γ_j. For the dipole radiation, we can get the angle distribution factor,

$$f(\theta_j, \phi_j) = \frac{I_j L^2 \cos\theta_j}{I_0 L^2 \cos 0} = \frac{\gamma_j \cos\theta_j}{\gamma_0}. \tag{S.4}$$

In spherical coordinates, $f(\theta_j, \phi_j) = 1 - \sin^2\theta_j \cos^2\phi_j$, where ϕ_j is the azimuth angle associated with the channel j[3]. Thus, γ_j can be obtained by

$$\gamma_j = \frac{\gamma_0}{\cos\theta_j}(1 - \sin^2\theta_j \cos^2\phi_j). \tag{S.5}$$

With the CMT in the free space[1], we can easily get the elements of $\boldsymbol{D}$,

$$\boldsymbol{D} = i\left(\sqrt{\frac{3\gamma_s(1-\sin^2\theta_1\cos^2\phi_1)}{2N_{3\mathrm{D}}\cos\theta_1}}, \sqrt{\frac{3\gamma_s(1-\sin^2\theta_2\cos^2\phi_2)}{2N_{3\mathrm{D}}\cos\theta_2}}, \cdots, \sqrt{\frac{3\gamma_s(1-\sin^2\theta_{N_{3\mathrm{D}}}\cos^2\phi_{N_{3\mathrm{D}}})}{2N_{3\mathrm{D}}\cos\theta_{N_{3\mathrm{D}}}}}\right)^T \tag{S.6}$$

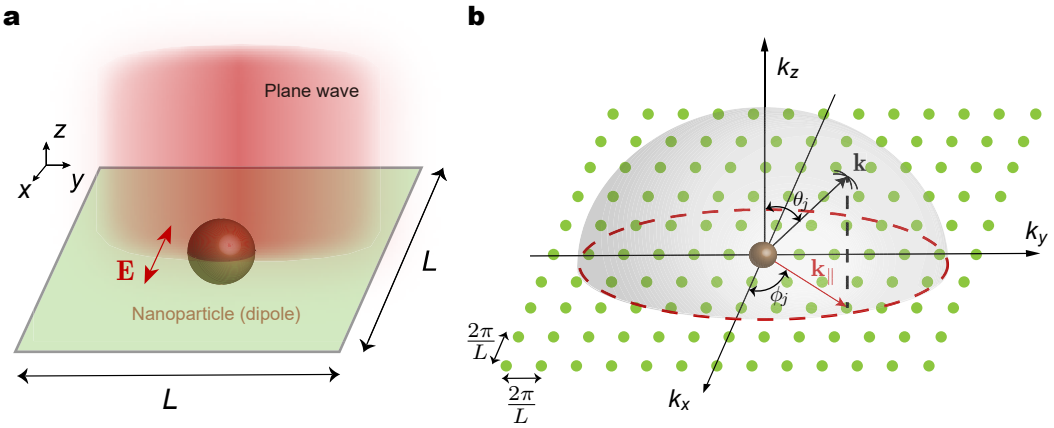

FIG. S1: (a) Schematic view of a resonator excited by a plane-wave illumination, which propagates along z-axis (green arrows) and polarizes along x-axis in the free space, $L \to \infty$ represents an infinitely large free space. (b) **k**-space containing a single nanoresonator with the scattering, and channels are represented by the dots in the projected k_{xy}-plane.

and $i=\sqrt{-1}$, the factor of 3/2 is a normalization factor, satisfying $\boldsymbol{D}^{+}\boldsymbol{D}=2\gamma_s$.

The absorption cross section of an electric dipole resonator thus can be calculated in the frequency domain as

$$\begin{aligned}
\sigma_a(\theta_j) &= \frac{\mathbf{S}_{\text{in}}^{*}\mathbf{S}_{\text{in}}-\mathbf{S}_{\text{out}}^{*}\mathbf{S}_{\text{out}}}{\mathbf{S}_{\text{in}}^{*}\mathbf{S}_{\text{in}}/L^2\cos\theta_j}=\frac{2\gamma_a a^{*}a}{\mathbf{S}_{\text{in}}^{*}\mathbf{S}_{\text{in}}/L^2\cos\theta_j}\\
&= \frac{1}{\mathbf{S}_{\text{in}}^{*}\mathbf{S}_{\text{in}}/L^2\cos\theta_j}\frac{2\gamma_a\mathbf{S}_{\text{in}}^{*}\boldsymbol{D}^{*}\boldsymbol{D}^{T}\mathbf{S}_{\text{in}}}{(\omega-\omega_0)^2+(\gamma_a+\gamma_s)^2}\\
&= \frac{3}{2N_{\text{3D}}}\frac{2\gamma_a\gamma_s}{(\omega-\omega_0)^2+(\gamma_a+\gamma_s)^2}L^2(1-\sin^2\theta_j\cos^2\phi_j)\\
&= \frac{3}{2\pi\lfloor nL/\lambda_0\rfloor^2}\frac{\gamma_a\gamma_s}{(\omega-\omega_0)^2+(\gamma_a+\gamma_s)^2}L^2(1-\sin^2\theta_j\cos^2\phi_j),\quad (L\to\infty)\\
&= \frac{3\lambda_0^2}{2\pi n^2}\frac{\gamma_a\gamma_s}{(\omega-\omega_0)^2+(\gamma_a+\gamma_s)^2}(1-\sin^2\theta_j\cos^2\phi_j).
\end{aligned}\tag{S.7}$$

which indicates the anisotropy of the dipole radiation. To maximize its absorption, θ_j is set to be 0 or π. The absoprtion cross section then can be written as

$$\sigma_a=\sigma_a(\theta_j)|_{\theta_j=0,\pi}=\frac{3\lambda_0^2}{2\pi n^2}\frac{\gamma_a\gamma_s}{(\omega-\omega_0)^2+(\gamma_a+\gamma_s)^2}.\tag{S.8}$$

Similarly, we can obtain the scattering cross section as

$$\begin{aligned}
\sigma_s(\theta_j) &= \frac{\mathbf{S}_{\text{out}}^{*}\mathbf{S}_{\text{out}}}{\mathbf{S}_{\text{in}}^{*}\mathbf{S}_{\text{in}}/L^2\cos\theta_j}=\frac{2\gamma_s a^{*}a}{\mathbf{S}_{\text{in}}^{*}\mathbf{S}_{\text{in}}/L^2\cos\theta_j},\quad (L\to\infty)\\
&= \frac{3\lambda_0^2}{2\pi n^2}\frac{\gamma_s^2}{(\omega-\omega_0)^2+(\gamma_a+\gamma_s)^2}(1-\sin^2\theta_j\cos^2\phi_j).
\end{aligned}\tag{S.9}$$

Then

$$\sigma_s=\sigma_s(\theta_j)|_{\theta_j=0,\pi}=\frac{3\lambda_0^2}{2\pi n^2}\frac{\gamma_s^2}{(\omega-\omega_0)^2+(\gamma_a+\gamma_s)^2}.\tag{S.10}$$

When $\omega=\omega_0,\gamma_a=\gamma_s$, the maximum of σ_a can be obtained as

$$\sigma_a^{\max}=\frac{3\lambda_0^2}{8\pi n^2}.\tag{S.11}$$

II. 2-dimensional case

The derivation of 2-dimensional absorption cross section of the electric dipole is almost similar to 3-dimensional case. It is worthy to note that the differences are the total number of channels N and the coupling rate γ_j. With regard to 2-dimension, the total number of channels is $N_{\text{2D}}=4\lfloor nL/\lambda_0\rfloor$. In polar coordinates, the angular distribution of radiation can be written as $f(\theta_j)=\cos^2\theta_j$. Hence, $\boldsymbol{D}$ becomes

$$\boldsymbol{D}=i\left(\sqrt{\frac{8\gamma_s\cos\theta_1}{N_{\text{2D}}\pi}},\sqrt{\frac{8\gamma_s\cos\theta_2}{N_{\text{2D}}\pi}},\cdots,\sqrt{\frac{8\gamma_s\cos\theta_{N_{\text{2D}}}}{N_{\text{2D}}\pi}}\right)^{T}.\tag{S.12}$$

Analogous to 3-dimensional case, the absorption cross section of a 2-dimensional dipole resonator is

$$\begin{aligned}
\sigma_a(\theta_j) &= \frac{2\gamma_a a^{*}a}{\mathbf{S}_{\text{in}}^{*}\mathbf{S}_{\text{in}}/L\cos\theta_j}\\
&= \frac{8}{\pi N_{\text{2D}}}\frac{2\gamma_a\gamma_s}{(\omega-\omega_0)^2+(\gamma_a+\gamma_s)^2}L\cos^2\theta_j\\
&= \frac{4}{4\pi\lfloor nL/\lambda_0\rfloor}\frac{4\gamma_a\gamma_s}{(\omega-\omega_0)^2+(\gamma_a+\gamma_s)^2}L\cos^2\theta_j,\quad (L\to\infty)\\
&= \frac{\lambda_0}{\pi n}\frac{4\gamma_a\gamma_s}{(\omega-\omega_0)^2+(\gamma_a+\gamma_s)^2}\cos^2\theta_j.
\end{aligned}\tag{S.13}$$

Then the absorption cross section of the 2-dimensional dipole becomes

$$\sigma_a = \sigma_a(\theta_j)|_{\theta_j=0,\pi} = \frac{\lambda_0}{\pi n}\frac{4\gamma_a\gamma_s}{(\omega-\omega_0)^2+(\gamma_a+\gamma_s)^2}. \tag{S.14}$$

Likewise, we can express the scattering cross section as

$$\sigma_s = \sigma_s(\theta_j)|_{\theta_j=0,\pi} = \frac{\lambda_0}{\pi n}\frac{4\gamma_s^2}{(\omega-\omega_0)^2+(\gamma_a+\gamma_s)^2}. \tag{S.15}$$

Also when $\omega=\omega_0, \gamma_a=\gamma_s$, the maximum of σ_a can be obtained as

$$\sigma_a^{\max} = \frac{\lambda_0}{\pi n}. \tag{S.16}$$

III. Derivation of σ_{a} with Mie Theory

For deep subwavelength nanoparticles, the geometric size (radius r) is much smaller than the resonant wavelength λ_0 ($r \ll \lambda_0$). Thus, only the lowest order plasmon resonance (electric dipole mode) could be able to be excited. Based on the Mie theory[4], it can be easily obtained that,

$$\sigma_s = \frac{3\lambda_0^2}{2\pi n^2}|a_1|^2,\ \sigma_e = \frac{3\lambda_0^2}{2\pi n^2}\mathrm{Re}(a_1), \tag{S.17}$$

$$\sigma_a = \sigma_e - \sigma_s = \frac{3\lambda_0^2}{2\pi n^2}(\mathrm{Re}(a_1) - \mathrm{Re}(a_1)^2 - \mathrm{Im}(a_1)^2). \tag{S.18}$$

where, σ_s, σ_e and σ_a are the scattering, extinction and absorption cross section respectively; λ_0 is light wavelength in vacuum; n is refractive index of the environmental medium and $a_1 = \mathrm{Re}(a_1)+i\mathrm{Im}(a_1)$ is Mie coefficient corresponding to the electric dipole component.

From Eq. (S.18), it can be easily shown that, a maximum σ_{a} would exist, when $\partial\sigma_a/\partial\mathrm{Re}(a_1)=0$ and $\partial\sigma_a/\partial\mathrm{Im}(a_1)=0$ are satisfied. Namely, $\sigma_a^{\max} = (3\lambda_0^2)/(8\pi n^2)$ corresponds to $a_1 = 0.5$. It is worthy to mention that, although the results shown are obtained for spherical particles, in principle, they would apply to any deep subwavelength particles of geometric shapes other than sphere.

IV. Obtaining γ_a and γ_s via Mie theory and CMT

From Eq. (S.8), (S.10) and the optical cross section calculated from Mie theory around the resonance wavelength of absorption, the ratio of scattering rate γ_s to absorption rate γ_a can be obtained. Meanwhile, the total decay rate is just the half widths at maximum (HWHMs), Γ^{HWHMs}, of the optical cross section spectra[5], namely,

$$\Gamma^{\mathrm{HWHMs}} = \gamma_a + \gamma_s. \tag{S.19}$$

By extracting the HWHMs from the absorption cross section spectra and solving Eq. (S.8), (S.10), the absorption rate γ_a and the scattering rate γ_s can be obtained readily.

V. Lorentz model of the gain materials

We use Lorentz model to describe the frequency dependent dielectric constant ε of the shell material with gain, i.e.

$$\varepsilon = \varepsilon_0 + (\varepsilon_{\mathrm{gain}}\omega_{\mathrm{gain}}^2)/(\omega_{\mathrm{gain}}^2 - \omega^2 - 2i\delta\omega). \tag{S.20}$$

For the case of gold core and dielectric shell, ε_0 is 2.56; ω_{gain} is set be to the frequency corresponding to the wavelength in vacuum around 530 nm; δ mainly influences the linewidth of the gain spectra, whose value is 9.01×10^{13} rad/s. And for two dimensional graphene nano-ribbon with upper and lower gain layers, ε_0 is also 2.56; the wavelength of ω_{gain} in vacuum is around 12.83 μm; δ is 2.86×10^{11} rad/s. By changing $\varepsilon_{\mathrm{gain}}$, the gain coefficient, $g = (4\pi/\lambda)\mathrm{Im}(\sqrt{\varepsilon})$, can be adjusted. It should be noted that for simplicity, the gain coefficient shown in the main text, typically corresponds to the maximum gain value at ω_{gain}.

VI. Maximizing absorption for a single spherical metal particle

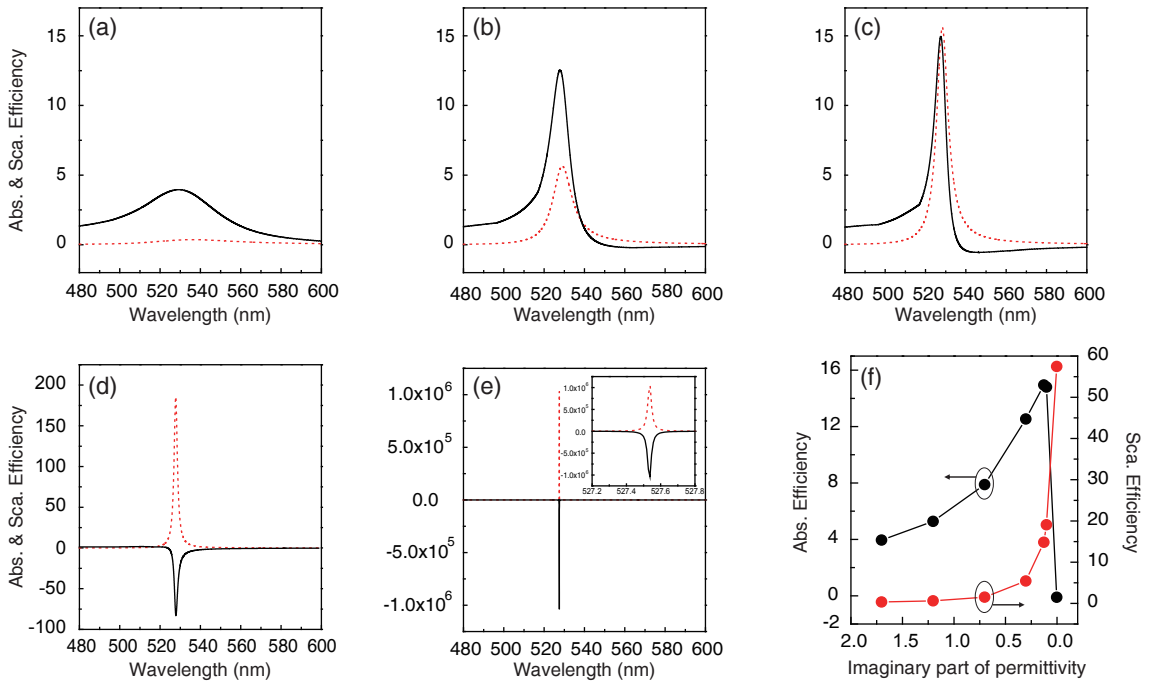

FIG. S2: (a-e) black curves correspond to the absorption efficiency, and red dash curves correspond to the scattering efficiency. From (a) to (e), the imaginary part values of permittivity of gold gradually decrease. And as an example, the imaginary part values at about 525.75 nm resonance wavelength are 1.7028, 0.7028, 0.1278, 0.0028 and -0.1332 respectively. The diameter of gold particle is 40 nm. Inset in (e): detailed spectra of (e) around resonant peak. (f) Peak value of absorption (black) and scattering (red) efficiency versus the imaginary part value at about 525.75 nm resonance wavelength.

In the main text, we propose that by introducing a gain medium in the structure, the absorption cross section of any deep subwavelength particle could be further boosted and even approach a maximum value. In this section, we want to show that the enhancement of absorption is not due to the effect of core-shell geometry. Here the gold sphere particle with diameter 40 nm without the dielectric shell immersed in water is considered , and we only decrease the imaginary part of the gold permittivity without changing the real part (Fig. S2). For a single spherical gold particle, its absorption efficiency is only 4, this result is trivial (Fig. S2(a)). When we decrease the imaginary part of the gold permittivity, the absorption efficiency increases at first (Fig. S2(a-c)) and then decreases (Fig. S2(c-e)), while the scattering efficiency continuously increases. This full process is similar to the case of using gain to increase absorption we shown in the main text. It is due to the fact that decreasing the imaginary part of the permittivity is equivalent to introducing gain to decrease absorption rate.

[1] M. Zhou, L. Shi, J. Zi and Z. Yu, Phys. Rev. Lett. **115**, 023903 (2015).
[2] E. Hecht, Optics, 3rd ed. (Addison Wesley, Bosten, 1997).
[3] J. D. Jackson, *Classical Electrodynamics*, 3rd ed. (Wiley, New York, 2001)
[4] C. F. Bohren and D. R. Huffman, *Absorption and Scattering of Light by Small Particles*, (Wiley-VCH, New York, 1998)
[5] R. E. Hamam, A. Karalis, J. D. Joannopoulos and M. Soljačić, Phys. Rev. A **75**, 053801 (2007).